

LIST OF APPENDICES

Appendix DR1. Methods	p. 1-2
Appendix DR2. Archival Data	p. 3
Hurricane Allen deposit (Figure DR1)	p. 3
Laguna Madre radiocarbon results (Table DR1)	p. 4
Late Holocene Gulf Coast intense hurricane probability plot (Figure DR2)	p. 5
Texas paleoclimate summary (Figure DR3)	p. 6
Error quantification (Figure DR4)	p. 7
Appendix DR3. Calculating $\langle h_b \rangle$	p. 8
Appendix DR4. Error analysis	p. 8-9
Appendix DR5. Total hurricane counts	p. 9
Appendix DR6. Radiocarbon reservoir effect	p. 9
References	p. 9-12

Appendix DR1. Methods

Thirty-seven 7.6 cm diameter vibracores up to 2m in length were collected for this study. Core locations were determined using a Garmin® hand-held GPS unit, which provided an approximate horizontal accuracy within 10 m. Mollusc shells were radiocarbon dated at the Keck Carbon Cycle AMS Facility at UC-Irvine. Radiocarbon ages were calibrated from radiocarbon to calendar years using Marine04 (Hughen et al., 2004) and IntCal04 (Reimer et al., 2004). All 554 samples were deflocculated in deionized water with a magnetic stirrer, and grain size measurements were performed using a Malvern Mastersizer 2000 particle analyzer. In core 32, the sediments below 146 cm were bioturbated and thus no washover deposits were identified below this depth. Grain size measurements were taken at 1 cm intervals from 80-147 cm in this core. Core Scientific International performed measurements of ^{137}Cs activity. Cesium samples

were taken approximately every 5 cm, so as to capture the age of the washover deposit in core 29.

Liu and Fearn (2000a) presented the lowermost age constraint of 3310 ± 80 ^{14}C yr B.P. from organic lake mud, and an uppermost age of 400 ^{14}C yr B.P. from the subsequent sedimentation age model. In order to directly compare all ages presented in this paper, these ages were calibrated using IntCal04 (Reimer et al., 2004) for terrestrial samples. The results of the calibration yield a lowermost age constraint of 3543 ± 90 yr B.P., and an uppermost age constraint of 492 ± 7 yr B.P.

Appendix DR2: Archival Data
Figure DR1- Hurricane Allen deposit

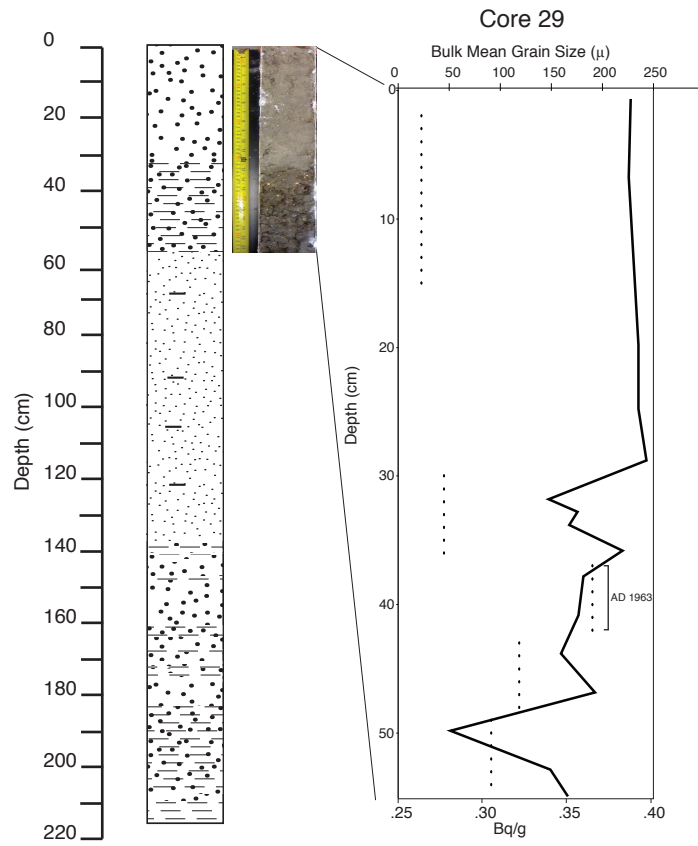


Table DR1: Laguna Madre radiocarbon results

Core	Sample name	$\delta^{13}\text{C}$ (‰)	^{14}C yr B.P.	Calibrated yr B.P. (1 sigma and 2 sigma)	Sample type	Sample depth (cm)
30	LM30-1_80-81	-1.9	2010 ± 15	1509-1654	bay mollusc shell	80-81
30	LM30-2_171-173	-0.3	4155 ± 15	4141-4329	bay mollusc shell	171-173
30	LM30-2_199-200	-0.7	4520 ± 15	4641-4808	bay mollusc shell	199-200
32	LM32-1_79-80.3	-1.0	2440 ± 15	2000-2143	bay mollusc shell	79-80.3
32	LM32-2_190-191.5**	-0.9	4620 ± 15	5308-5445	bay mollusc shell	190-191.5
32	LM32-2_195-197	-0.8	5115 ± 15	5438-5559	bay mollusc shell	195-197
25	LM25_127cm	0.9	1885± 20	1362-1503	shell (<i>m. lateralis</i> and <i>P. multilineata</i>)	127
25	LM25_154-158cm	-0.7	2260± 15	1830-1895	shell fragments	154-158
25	LM25_180-182cm	0.4	2685 ± 20	2315-2448	shell (<i>P. multilineata</i>) and fragments	180-182
33	LM33_83cm	0.0	1390± 15	890-989	shell (<i>P. multilineata</i>)	83
33	LM33_96cm*	0.6	1130± 15	644-721	shell (<i>E. concentracia</i>)	96
33	LM33_167cm**	-2.2	3335± 15	3484-3632	shell (<i>P. multilineata</i>)	167

*too young based on older date from *Parvilucina multilineata* shell above

**IntCal04 (Reimer et al., 2004) was used to calibrate due to possible fluvial influence

Figure DR2-Late Holocene Gulf Coast intense hurricane probability plot

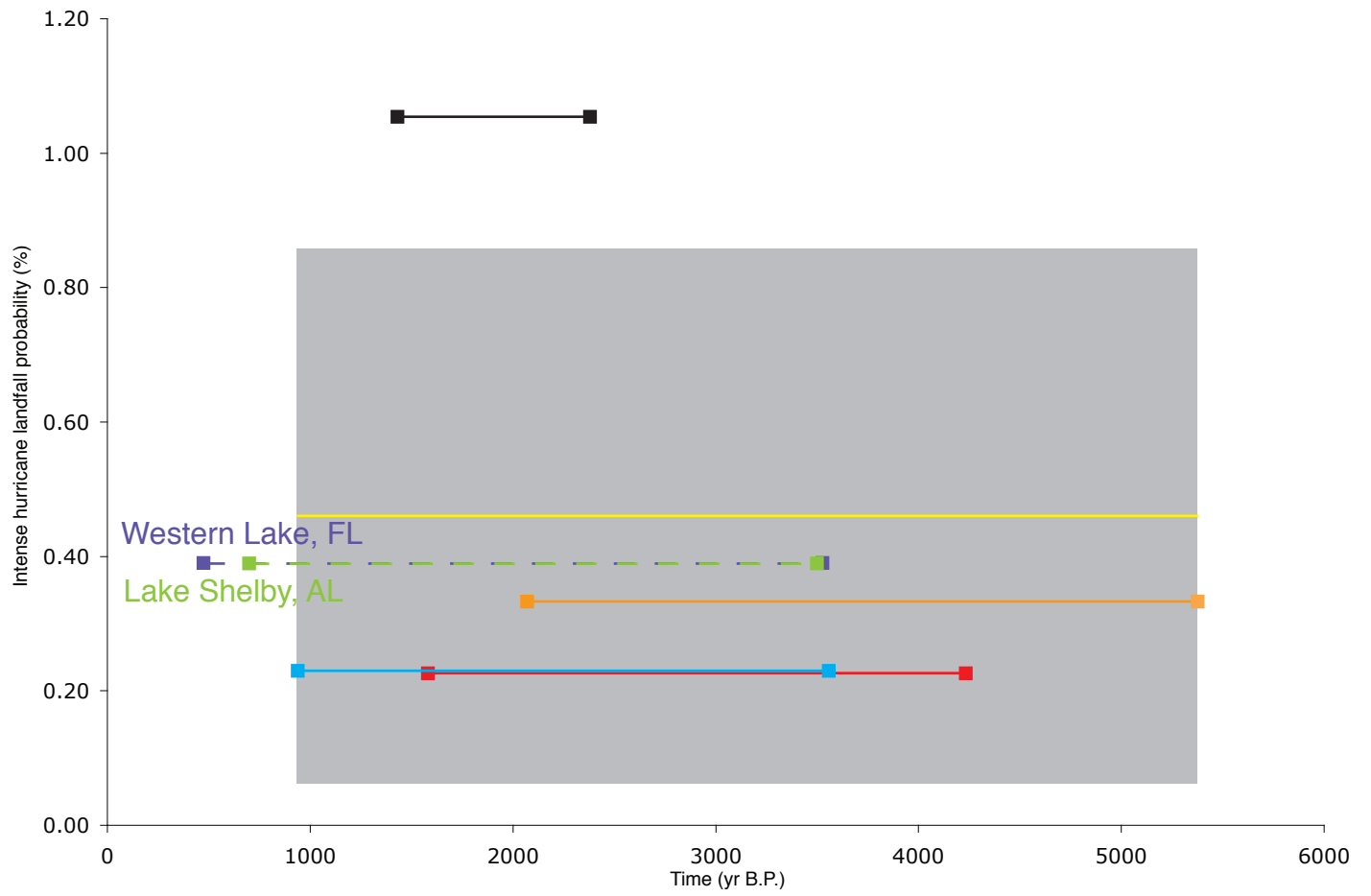


Figure DR3- Texas paleoclimate summary

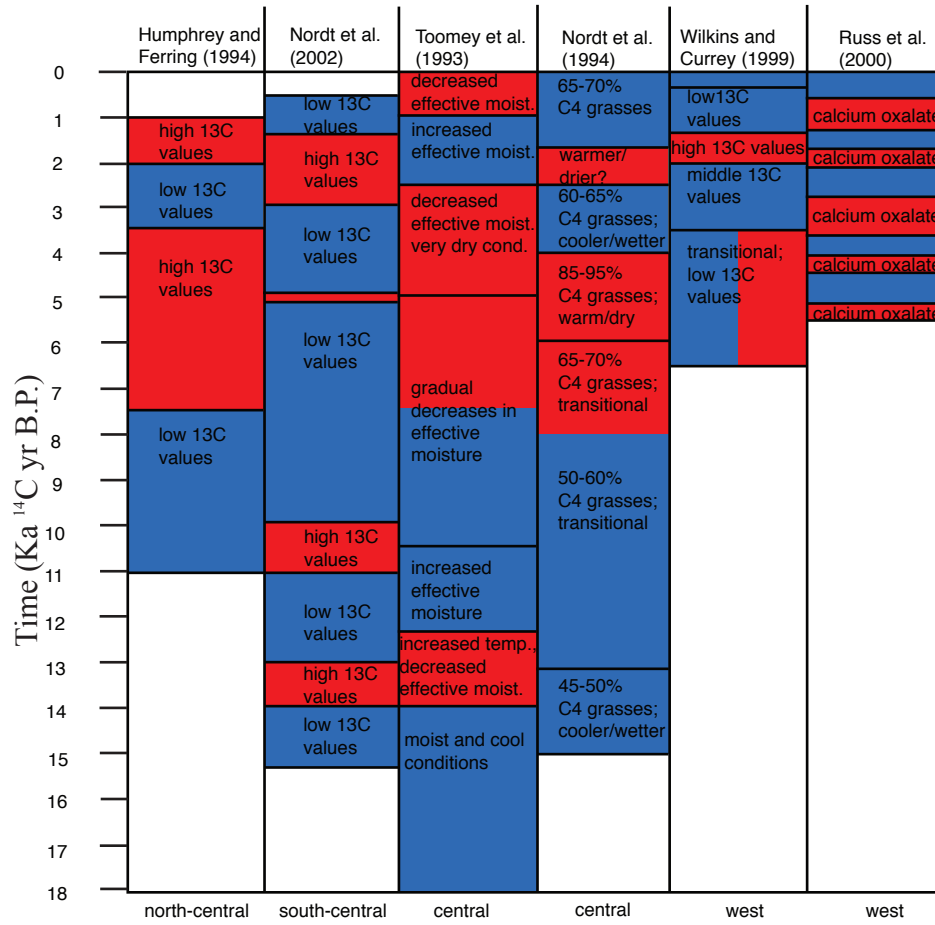
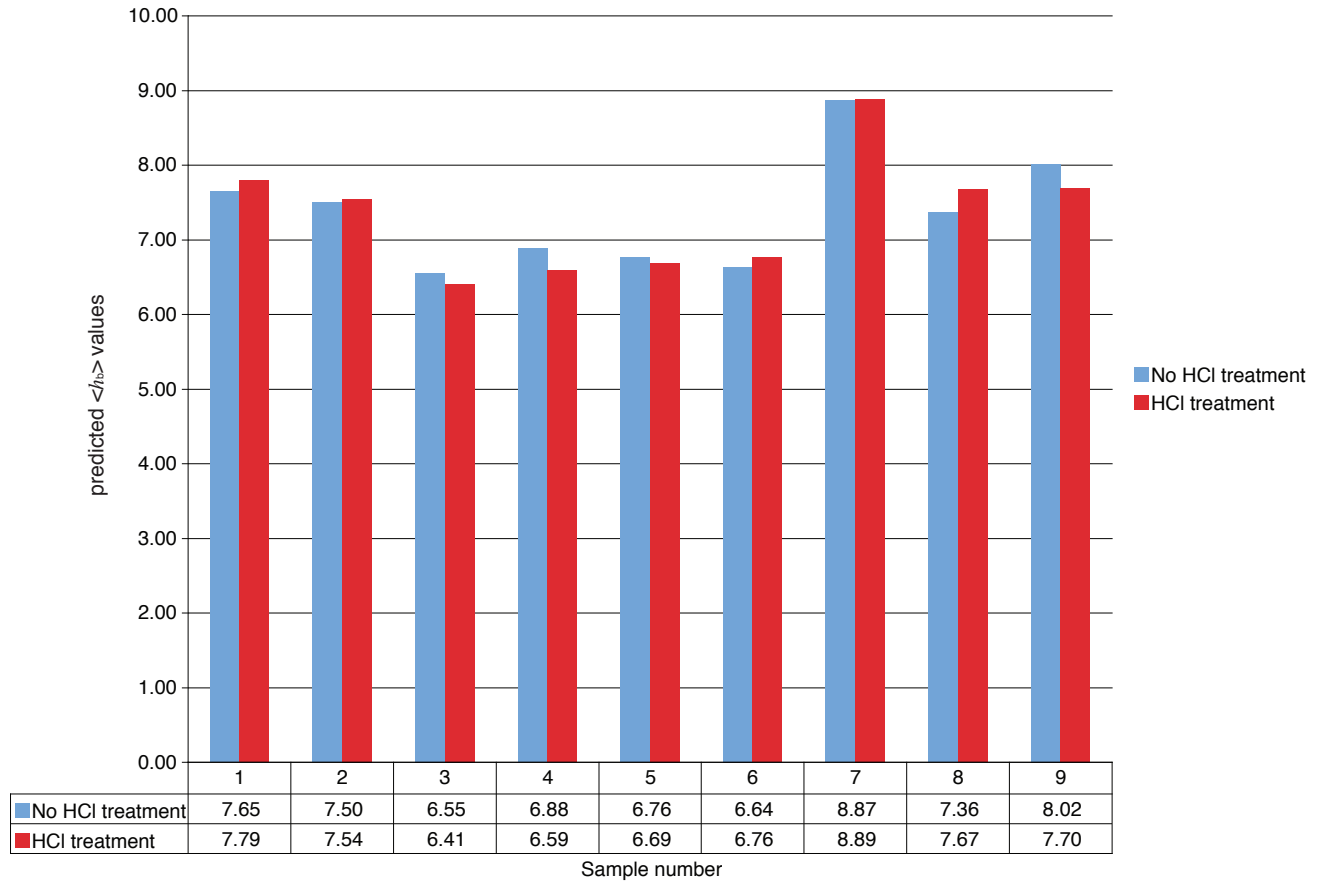


Figure DR4- Error quantification



sample #	w_s (m/s)	x_L (m/s)	$\langle h \rangle$ (m)	Sample ID	Bulk mean grain size (μ)
No HCl treatment					
1	0.03	2157	7.65	LM25_069	235.13
2	0.03	2157	7.50	LM25_102	229.99
3	0.03	1750	6.55	LM29_10	231.25
4	0.03	1750	6.88	LM29_26	244.03
5	0.02	2274	6.76	LM30_130	198.43
6	0.02	2274	6.64	LM30_136	194.62
7	0.02	3567	8.87	LM32_087	192.48
8	0.03	2393	7.36	LM33_73	209.34
9	0.03	2393	8.02	LM33_80	229.54
HCl treatment					
1	0.03	2157	7.79	LM25_069	240.11
2	0.03	2157	7.54	LM25_102	231.43
3	0.03	1750	6.41	LM29_10	225.59
4	0.03	1750	6.59	LM29_26	232.67
5	0.02	2274	6.69	LM30_130	196.17
6	0.02	2274	6.76	LM30_136	198.44
7	0.02	3567	8.89	LM32_087	192.92
8	0.03	2393	7.67	LM33_73	218.70
9	0.03	2393	7.70	LM33_80	219.57

Appendix DR3. Calculating $\langle h_b \rangle$

A storm's flow depth over the barrier ($\langle h_b \rangle$) can be calculated (Woodruff et al., 2008):

$$\langle h_b \rangle = \left(\frac{x_L^2 w_s^2}{g} \right)^{1/3}, \quad (3.1)$$

where, x_L = the distance at which inundating currents transport a suspended particle a horizontal distance into the lagoon, w_s = particle settling velocity, and g = acceleration due to gravity. w_s was calculated using a recently derived universal equation for sediment fall velocities (Ferguson and Church, 2004):

$$w_s = \frac{RgD^2}{C_1\nu + (0.75C_2RgD^3)^{0.5}}, \quad (3.2)$$

where R = the submerged specific gravity (1.65 for quartz), g = the acceleration due to gravity, D = grain diameter, C_1 = constant with value of 18 for grains of varied shape, ν = the kinematic viscosity of the fluid ($9.2 \times 10^{-7} \text{ m}^2\text{s}^{-1}$), and C_2 = constant with value of 1 for grains of varied shape. For each discrete storm bed, the bulk mean grain size ($(\phi_{16} + \phi_{50} + \phi_{84})/3$) was used to determine w_s , followed by $\langle h_b \rangle$.

Appendix DR4. Error analysis

Shell material was avoided during grain size measurements. However, in order to quantify potential error from carbonate material in the calculation of $\langle h_b \rangle$, representative samples from washover sands were taken from each core. One was treated with HCl to dissolve all shell material, while the other was left untreated. Both samples were then analyzed for grain size, and potential errors for predicted $\langle h_b \rangle$ values for each sample were calculated based on the grain size

differences. These errors appear to be negligible, and there is no evidence that shell material is abundant enough to shift the bulk mean grain size towards the coarser fraction (Figure DR4).

Appendix DR5. Total hurricane counts

We classify hurricanes as intense using the predicted $\langle h_b \rangle$ value from Hurricane Allen as a baseline. If the total number of storms is used for each probability calculation regardless of the predicted $\langle h_b \rangle$ value, the probabilities change slightly. Ten total hurricane events are recorded from 4,235–1,582 yr B.P. (0.38% landfall probability) in core 30, eleven from 2,382–1,433 yr B.P. (1.16% landfall probability) in core 25, sixteen are recorded from 3,558–940 yr B.P. (0.61% landfall probability) in core 33, and a total of twelve from 5,377–2,072 yr B.P. (0.36% landfall probability) in core 32 (Fig. 2). The average landfall probability of these values is $\sim 0.63\%$ (with a standard deviation value of $\pm 0.37\%$)

Appendix DR6. Radiocarbon reservoir effect

Along the Texas coast, a recent study has quantified radiocarbon reservoirs associated with organisms utilizing CO₂ which has not been in contact with the atmosphere for long periods of time (Milliken et al., 2008). This study concluded that the reservoir increases from west to east in Texas, and ranges from ~ 400 -700 yrs. No reservoir data currently exists for LM. However, given the extremely limited exchange between LM, fluvial systems, and the Gulf of Mexico, this effect is likely to be negligible. Therefore, the standard ~ 400 -year global average reservoir is used (Marine04-Hughen et al., 2004).

References:

Ferguson, R.I., and Church, M., 2004, A simple universal equation for grain settling velocity:
Journal of Sedimentary Research, v. 74, p. 933-937.

Hughen, K.A., Baillie, M.G.L., Bard, B.E., Beck, J.W., Bertand, C.J.H., Blackwell, P.G., Buck, C.E., Burr, G.S., Cutler, K.B., Damon, P.E., Edwards, R.L., Fairbanks, R.G., Friedrich, M., Guilderson, T.P., Kromer, B., McCormac, G., Manning, S., Ramsey, C.B., Reimer, P.J., Reimer, R.W., Remmele, S., Southon, J.R., Stuiver, M., Talamo, S., Taylor, F.W., van der Plicht, J. and Weyhenmeyer, C.E., 2004, Marine04 Marine radiocarbon age calibration, 0–26 ka BP: *Radiocarbon*, v. 46, p. 1059–1086.

Humphrey, J.D., and Ferring, C.R., 1994, Stable Isotopic Evidence for Latest Pleistocene and Holocene Climatic Change in North-Central Texas: *Quaternary Research*, v. 41, p. 200-213.

Liu, K.B., and Fearn, M.L., 2000a, Reconstruction of prehistoric landfall frequencies of catastrophic hurricanes in northwestern Florida from lake sediment records: *Quaternary Research*, v. 54, p. 238-245.

Liu, K.B., and Fearn, M.L., 2000b, Holocene history of catastrophic hurricane landfalls along the Gulf of Mexico coast reconstructed from coastal lake and marsh sediments, *in* Ning, Z.H., Abdollahi, K.K., eds., *Current Stresses and Potential Vulnerabilities: Implications of Global Change for the Gulf Coast Region of the United States*: Baton Rouge, Gulf Coast Regional Climate Change Council, p. 38-47.

Maddox, J.K., 2005, *Holocene Evolution of the Matagorda/Lavaca Bay Complex, Central Texas Coast* [M.S. thesis], Houston, Rice University, 124 p.

Milliken, K.T., Anderson, J.B., Rodriguez, A.B., 2008, A new composite Holocene sea-level curve for the northern Gulf of Mexico: *Geological Society of America, Special Paper 443*, p. 1-11.

- Nordt, L.C., Boutton, T.W., Jacob, J.S., and Mandel, R.D., 2002, C₄ plant productivity and climate-CO₂ variations in south-central Texas during the Late Quaternary: *Quaternary Research*, v. 58, p. 182-188.
- Nordt, L.C., Boutton, T.W., Hallmark, C.T., and Waters, M.R., 1994, Late Quaternary Vegetation and Climate Changes in Central Texas Based on the Isotope Composition of Organic Carbon: *Quaternary Research*, v. 41, p. 109-120.
- Reimer, P.J., Baillie, M.G.L., Bard, E., Bayliss, A., Beck, J.W., Bertrand, C.J.H., Blackwell, P.G., Buck, C.E., Burr, G.S., Cutler, K.B., Damon, P.E., Edwards, R.L., Fairbanks, R.G., Friedrich, M., Guilderson, T.P., Hogg, A.G., Hughen, K.A., Kromer, B., McCormac, G., Manning, S., Ramsey, C.B., Reimer, R.W., Remmele, S., Southon, J.R., Stuiver, M., Talamo, S., Taylor, F.W., van der Plicht, J., and Weyhenmeyer, C.E., 2004, IntCal04 Terrestrial radiocarbon age calibration, 0–26 ka BP: *Radiocarbon*, v. 46, p. 1029–1058.
- Roth, D., 2000, Texas Hurricane History: <http://www.srh.noaa.gov/lch/research/txhur.php> (September 2009).
- Russ, J., Loyd, D.H., Boutton, T.W., 2000, A paleoclimate reconstruction for southwestern Texas using oxalate residue from lichen as a paleoclimate proxy: *Quaternary International*, v. 67, p. 29-36.
- Toomey, R.S., III, Blum, M.D., and Valastro, S., Jr., 1993, Late Quaternary climates and environments of the Edwards Plateau, Texas: *Global and Planetary Change*, v. 7, p. 299-320.
- Wilkins, D.E., and Currey, D.R., 1999, Radiocarbon chronology and ¹³C analysis of mid- to late-Holocene Aeolian environments, Guadalupe Mountains National Park, Texas, USA: *The Holocene*, v. 9, no. 3, p. 363-371.

Woodruff, J.D., Donnelly, J.P., Mohrig, D., Geyer, W.R., 2008, Reconstructing relative flooding intensities responsible for hurricane-induced deposits from Laguna Playa Grande, Vieques, Puerto Rico: *Geology*, v. 36, p. 391-394, doi:10.1130/G24731A.1.

FIGURE CAPTIONS

Figure DR1- Hurricane Allen deposit

Lithology and bulk mean grain size of core 29. Note the ~30 cm thick clean sand deposit at the top of the core, attributed to Hurricane Allen (1980). This core was dated using ^{137}Cs (black circles), and yielded a cesium spike (indicating AD 1963 \pm 2) at ~38 cm depth. The predicted $\langle h_b \rangle$ value for this deposit was 6.6 m, while the measured surges were 3.7 m (Roth, 2000). The highest surges occurred in uninhabited areas and were not measured. The predicted $\langle h_b \rangle$ value from this event was used as a baseline to constrain intense storms. Lithologic legend in Fig. 2.

Figure DR2- Late Holocene Gulf Coast intense hurricane probability plot

Plot showing intense hurricane landfall probabilities between paleotempestological studies from Lake Shelby, AL (Liu and Fearn, 2000b – dashed green), Western Lake, FL (Liu and Fearn, 2000a-dashed purple), and Laguna Madre (LM), TX (solid black, orange, blue, red). X-axis is calibrated radiocarbon age intervals. Yellow line represents the average landfall probability (0.46%) between cores from LM, and the grey box represents \pm one standard deviation from the average landfall probability between cores from LM. Note the similar intense hurricane landfall probabilities and time intervals between sites.

Figure DR3- Texas paleoclimate summary

Compilation of climate studies for the past ~18,000 years (modified from Maddox, 2005). Red represents warm, dry conditions, and blue represents cool, wet conditions. Texas regional location indicated at bottom of each study.

Figure DR4- Error analysis

Comparison of representative washover samples with and without HCl treatment from all cores.

There is little variability in predicted $\langle h_b \rangle$ values between treated and untreated samples.

¹GSA Data Repository item 2010149, Appendices DR1–DR6 (methods, archival data, calculating $\langle h_b \rangle$, error quantification, and radiocarbon reservoir effect), is available online at www.geosociety.org/pubs/ft2010.htm, or on request from editing@geosociety.org or Documents Secretary, GSA, P.O. Box 9140, Boulder, CO 80301, USA.